Clinical Neurophysiology 132 (2021) 1636–1646

Contents lists available at ScienceDirect

Clinical Neurophysiology

journal homepage: www.elsevier.com/locate/clinph

Monitoring anesthesia using simultaneous functional Near Infrared Spectroscopy and Electroencephalography

Vidhya Vijayakrishnan Nair [a], Brianna R. Kish [a], Ho-Ching (Shawn) Yang [a], Zhenyang Yu [b], Hang Guo [c], Yunjie Tong [a,*], Zhenhu Liang [b]

[a] Weldon School of Biomedical Engineering, Purdue University, West Lafayette, IN, United States
[b] School of Electrical Engineering, Yanshan University, Qinhuangdao, China
[c] Department of Anesthesiology, the Seventh Medical Center to Chinese PLA General Hospital, Beijing 100700, China

ARTICLE INFO

Article history:
Accepted 28 March 2021
Available online 17 April 2021

Keywords:
General Anesthesia
Functional Near Infrared Spectroscopy
Electroencephalography

HIGHLIGHTS

- The anesthesia maintenance phase is characterized by a significant decrease in the complexity and power of cerebral hemodynamic signals.
- Adults exhibit a higher coupling between low frequency oscillations (0.01–0.1 Hz) in fNIRS and EEG as compared to children.
- fNIRS offers a complementary neurovascular assessment to EEG that improves the accuracy of anesthesia monitoring.

ABSTRACT

Objective: This study aims to understand the neural and hemodynamic responses during general anesthesia in order to develop a comprehensive multimodal anesthesia depth monitor using simultaneous functional Near Infrared Spectroscopy (fNIRS) and Electroencephalogram (EEG).
Methods: 37 adults and 17 children were monitored with simultaneous fNIRS and EEG, during the complete general anesthesia process. The coupling of fNIRS signals with neuronal signals (EEG) was calculated. Measures of complexity (sample entropy) and phase difference were also quantified from fNIRS signals to identify unique fNIRS based biomarkers of general anesthesia.
Results: A significant decrease in the complexity and power of fNIRS signals characterize the anesthesia maintenance phase. Furthermore, responses to anesthesia vary between adults and children in terms of neurovascular coupling and frontal EEG alpha power.
Conclusions: This study shows that fNIRS signals could reliably quantify the underlying neuronal activity under general anesthesia and clearly distinguish the different phases throughout the procedure in adults and children (with less accuracy).
Significance: A multimodal approach incorporating the specific differences between age groups, provides a reliable measure of anesthesia depth.

1. Introduction

General anesthesia can be described as a drug-induced, reversible state of unconsciousness, during which the patient is immobile, retains no memory, and experiences no pain. Under general anesthesia there is a strict, stable maintenance of the autonomic, cardiovascular, respiratory, and thermoregulatory systems (Brown et al., 2018, 2010). Balanced general anesthesia, as it is commonly practiced today, involves the administration of multiple drugs to create and maintain the anesthetic state (Brown et al., 2018), so as to safely perform surgical and non-surgical procedures (Purdon et al., 2013). 8 percent of the world's population every year receives general anesthesia at least once (Hernandez-Meza et al., 2018). In the United States alone, 60,000 patients are put under general anesthesia every day (Brown et al., 2010), however, there lacks a reliable benchmark system for monitoring the deliv-

* Corresponding author.
E-mail address: tong61@purdue.edu (Y. Tong).

https://doi.org/10.1016/j.clinph.2021.03.025
1388-2457/

ery and maintenance of anesthesia. Currently, anesthesiologists primarily rely on peripheral measurements, such as heart rate, respiration rate, oxygen saturation, and end-tidal anesthetic concentration, along with the clinical status of the patient, to determine the drugs and ideal dosage for each case and quantify the patient's anesthesia depth throughout the procedure (Hernandez-Meza et al., 2017).

A well-founded anesthesia depth monitoring technique that directly reflects the brain state is therefore essential, as both insufficient and excessive dosage could lead to serious complications. An inadequate anesthesia depth can lead to intraoperative awareness, including auditory and tactile perception, followed by feelings of helplessness, immobility, pain, and panic, as well as an acute fear of death. Previous research has reported that it might also lead to the development of post-traumatic stress disorder with symptoms such as anxiety, insomnia, nightmares, irritability, depression and potential suicidality (Bischoff and Rundshagen, 2011; Kent et al., 2013). On the other hand, an anesthetic overdose could lead to delayed post-operative recovery (Sinclair and Faleiro, 2006), neurological complications/injury, cardiovascular complications (Giraldo et al., 2018) and even death (Li et al., 2009).

In recent decades, advances in anesthesia monitoring used in clinical practice include the electroencephalogram (EEG) based Bispectral index (BIS) monitor (Medtronic, Dublin, Ireland) and M−entropy (GE Healthcare, Helsinki, Finland) (Bruhn et al., 2006; Viertio-Oja et al., 2004). However, the widespread use of these monitors is limited, with routine use in an estimated 1.8 percent of all surgical/non-surgical procedures (Avidan and Mashour, 2013). This can be attributed to known variability of their performance under opioid drugs (Manyam et al., 2007), inadequate prediction of emergence from anesthesia (Ishioka et al., 2017), decreased capability in preventing intraoperative awareness (Avidan et al., 2011), and no significant improvements in the quality of post-operative recovery (Leslie et al., 2005) and early and intermediate-term survival (Leslie et al., 2010). Furthermore, EEG based BIS measures are also susceptible to high frequency noise from electro-surgical devices, making them invalid during their use (Wang et al., 2020).

In addition, anesthetic drug specific changes in the power and coherence of different frequencies in raw EEG signals have been reported (Akeju et al., 2014; Hagihira, 2015; Hight et al., 2017; Purdon et al., 2015, 2013). A recent study has also found that anesthesia induced EEG oscillations illustrate age-dependence (Lee et al., 2017). However, the problem with these established EEG signatures is that they only reverse significantly after the patient recovers consciousness, hence limiting their potential as a standalone measure of anesthesia depth.

Furthermore, reliable monitoring of all phases of general anesthesia cannot be accomplished with only EEG indices, since anesthesia induces a spectrum of both neural and hemodynamic changes specific to the type of drug (Shalbaf et al., 2014).

This situation has prompted research into the capabilities of alternative modalities, particularly functional Near Infrared Spectroscopy (fNIRS), to identify biomarkers specific to the anesthetic drug action. fNIRS is a non-invasive optical imaging device that can be easily adapted to the operating room. Unlike EEG, fNIRS is sensitive to the concentration changes of oxyhemoglobin (Δ[HbO]) and deoxyhemoglobin (Δ[Hb]). As a result, fNIRS can measure neuronal signals through neurovascular coupling (Ferrari and Quaresima, 2012), which can offer complementary information about anesthesia depth. fNIRS has been used previously to characterize the depths of anesthesia. The changes in Δ[HbO], Δ[Hb] and total hemoglobin (Δ[HbT]) during the transitions have been used to distinguish the maintenance phase of anesthesia (Hernandez-Meza et al., 2018, 2017; Izzetoglu et al., 2011; Leon-Dominguez et al., 2014; Liang et al., 2016). However, robust fNIRS based biomarkers that directly relate to the underlying the neuronal activity specific to all stages of the general anesthesia process have not yet been reliably quantified.

The goal of this concurrent fNIRS and EEG study is to 1) compare the signals from these two modalities during the whole procedure of general anesthesia to examine the coupling between neuronal and neurovascular responses; 2) develop reliable imaging biomarkers based on fNIRS or fNIRS/EEG, to distinguish the different phases of general anesthesia.

2. Methods

2.1. Patients

A total of 54 surgery patients admitted to PLA Army General Hospital, Beijing, China, who had undergone general anesthesia during various surgeries were analyzed in this retrospective study. The protocol was approved by the Institutional Review Board of the Seventh Medical Center to Chinese PLA General Hospital. Written informed consent was obtained from all adult patients or parent (s) of pediatric patients. The surgeries included circumcision, multi-finger amputation, ureteroscopy, knee arthroscopy, ureteral lithotripsy, laparoscopic cholecystectomy, and cystoscopy. All patients maintained a supine position throughout the procedure. The patients included two age groups: (i) 18 – 60 years (n = 37, 14 females and 23 males, mean age = 32.49 ± 10.58 years) and (ii) 6 – 10 years (n = 17, 3 females and 14 males, mean age = 7.2 6 ± 1.28 years). All patients enrolled in the study were classified as American Society of Anesthesiologists physical status I or II.

2.2. Anesthetic drugs and timeline of measurement

Intravenous infusion of propofol was used to induce general anesthesia in all the patients enrolled in the study. Propofol exercises its primary hypnotic and sedative effects by potentiating specific γ-aminobutyric acid type A receptor subtype ($GABA_A$ receptor) mediated inhibition of impulses in the neural network in the brain (Khan et al., 2014; Rudolph and Antkowiak, 2004). The general anesthesia was maintained with sevoflurane, a halogenated inhalational agent, with agonist effects at $GABA_A$ and glycine receptors. Sevoflurane also inhibits excitatory synaptic channel activity in the central nervous system, with its antagonistic effects on N-methyl-D-aspartate (NMDA), nicotinic acetylcholine, serotonin, and glutamate receptors (Franks, 2008). Patients were also administered either fentanyl or sufentanil for intraoperative analgesia and cisatracurium or rocuronium for relaxation of skeletal muscles. Fentanyl and sufentanil are lipid soluble μ-opioid receptor agonists, with similar onset times, but sufentanil has a shorter duration of action (Sear, 1998). Cisatracurium and rocuronium are both non-depolarizing neuromuscular blocking agents, primarily used to facilitate tracheal intubation. They bind to the nicotinic cholinergic receptors at the muscle motor end-plate to exert their effects (Naguib et al., 1998; Strawbridge et al., 2020). In addition, most of the patients were also given midazolam for its sedative, anxiolytic and amnestic effects before the induction of general anesthesia (Oxorn et al., 1997; Reves et al., 1985).

The timeline of fNIRS and EEG measurement during the surgery is depicted in Fig. 1. For this study, the timeline of measurement has been divided into four phases of interest: Wakefulness, Maintenance, Recovery and after recovery of consciousness (ROC). Before the infusion of anesthetic drugs, the patients were pre-oxygenated with 40–50 percent oxygen (flow = 2 L/min) and received midazolam as a pre-medication. The induction of anesthesia begins with an intravenous infusion of propofol. During this

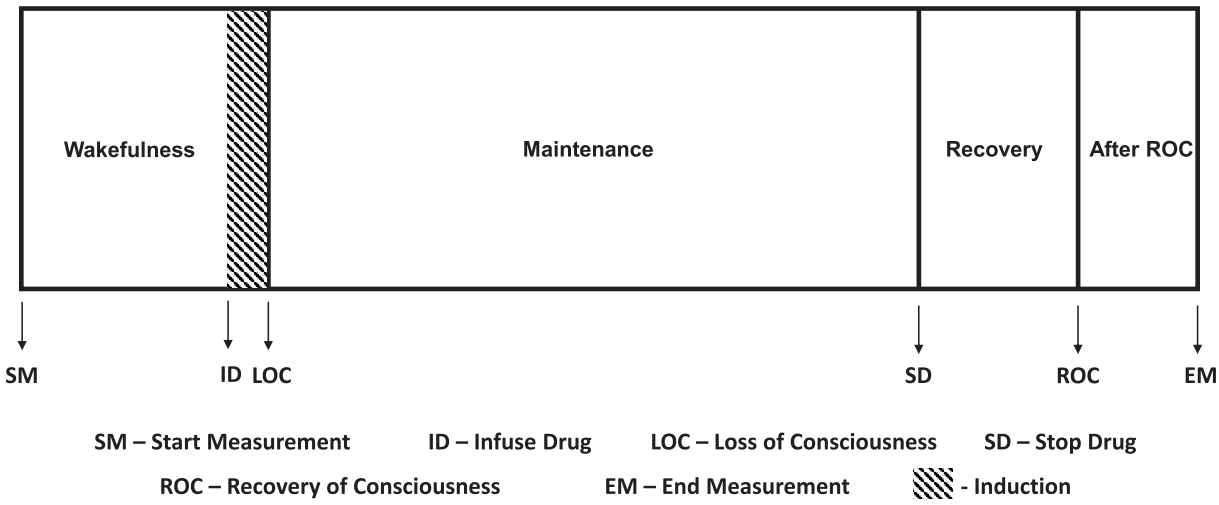

Fig. 1. Phases of interest with reference to the surgery/measurement timeline.

time, they were asked to repeat their names every ten seconds by the anesthesiologist. The time point at which they failed to respond to the verbal command was marked as the LOC (loss of consciousness) time point. After the loss of consciousness, the neuromuscular blocking agent (cisatracurium or rocuronium) was administered. The airway was maintained with tracheal intubation or by the placement of a laryngeal mask airway. Anesthesia depth was maintained with sevoflurane, and a bolus of intravenous propofol was administered when the sedation of the patient was determined insufficient by the anesthesiologist. The dose of sevoflurane ranged between 0.5 % and 4%, in order to ensure a reasonable depth of anesthesia during maintenance. During this phase, patients were also administered analgesic agents (fentanyl or sufentanil) and supplementary doses of cisatracurium or rocuronium to maintain the required levels of muscle relaxation. The recovery phase is defined as the time period from the cessation of drug infusion to the recovery of consciousness. The administration of anesthetic agents, analgesic agents and neuromuscular blocking agents was terminated during the beginning of this phase. The anesthetic drugs are washed out from the patient's body during this phase, which leads to the recovery of consciousness, confirmed by purposeful movement at the end of recovery phase. More specifically, during this time, they were asked to move their right hand every 10 seconds. When the patients correctly responded to the verbal command, the corresponding time point was recorded as the ROC (Recovery of consciousness) time point.

2.3. Data collection

2.3.1. fNIRS description

fNIRS is a non-invasive, non-ionizing optical neuroimaging technology widely used to investigate the hemodynamics of the healthy brain and a multitude of brain pathologies (Boas et al., 2014; Ferrari and Quaresima, 2012). In this study, the fNIRS data was collected using two different fNIRS devices:

(i) The CW NIRS system (NIRx; Berlin, Germany) with 10 m long optical fibers and LED sources, each combining two wavelengths (760 and 850 nm). The source-detector distance was set to 3 cm. The CW NIRS system with a sampling rate of 7.8125 Hz was used to measure the relative Δ[HbO] and Δ[Hb] changes of 15 patients in the age group of 18–60 years.

(ii) The EGOS-600A (EnginMed, Co., Ltd. Suzhou, China) with four channels, each connected to a tissue oxygen probe of length 3 m. Each probe has 1 source and 2 detectors, with the source-detector distances of 3 cm and 4 cm. The probe's light source has three wavelengths (760 nm, 810 nm, and 850 nm). For this study, only two channels were used to record the cortical blood oxygen changes from the remaining patients enrolled, at a sampling rate of 1 Hz. The spatially resolved spectroscopy (SRS) algorithm was used to calculate the changes in Δ[HbO], Δ[Hb] and total hemoglobin values.

The source-detector configuration and placement of sensors from both EGOS-600A and NIRX CW NIRS systems are illustrated in Fig. 2a and 2b, respectively. The sensors were placed on the forehead of the patients in such a way that the two channels captured the neurovascular changes in the right and left prefrontal cortex of the brain (Fp1 and Fp2).

2.3.2. EEG description

Two-channel frontal EEG was recorded during surgery using a BIS monitor (Medtronic, USA). The sampling rate was 128 Hz per channel. The BIS electrode array was recorded from approximately FPz-F9 (International 10–20 system) and FPz-AF7. The electrode impedance was less than 5 kΩ for each channel. These two EEG recordings covered the same hemisphere of the brain. In this study, we only analyzed the EEG from FPz-F9.

2.4. Data screening and processing

2.4.1. fNIRS

The fNIRS data screening and processing were carried out using MATLAB (MATLAB 2015b, The MathWorks Inc., Natick, MA, 2000). The Δ[HbO] and Δ[Hb] data from each channel of every subject were visually inspected and those identified with motion artifacts were corrected using a correlation-based signal improvement technique (Cui et al., 2010). Δ[HbO] and Δ[Hb] signals from the two channels of fNIRS exhibited a very high correlation of 0.72 ± 0.25 and 0.78 ± 0.24. This implies that there is no significant difference in hemodynamic responses between the left and right prefrontal cortex due to the global effect of general anesthesia. All further analyses were carried out after averaging the responses from the fNIRS channels for each subject to increase the signal–noise-ratio.

Spectrogram: A time–frequency analysis was then performed on the motion-corrected signals, using the spectrogram function (spectrogram from MATLAB, window type = hamming, window length = 100 seconds, overlap = 90 percent, sampling points (nfft) = sampling frequency/frequency resolution), with a window

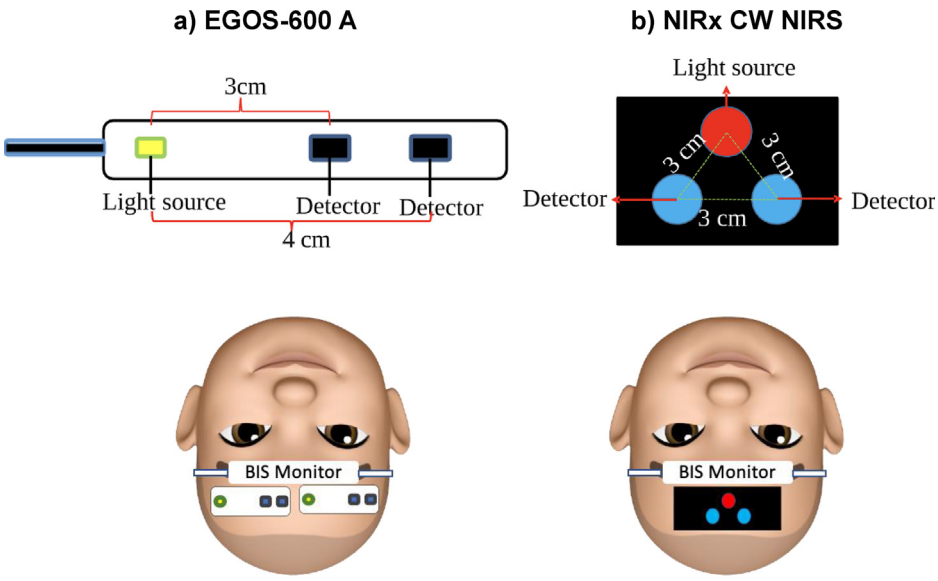

Fig. 2. Source – detector configuration of functional Near Infrared Spectroscopy (fNIRS) channels and placement of fNIRS probes on patient head for a) EGOS-600 A and b) NIRx CW NIRS systems.

length of 100 seconds and an overlap of 90 percent, to visualize the variations in the frequency spectrum over the entire duration of anesthesia. A window length of 100 sec gives a frequency bin width of 0.01, thereby potentially eliminating oscillations less than 0.01 Hz, from the spectrum. Also, an overlap of 90 percent gives a time resolution of 10 seconds, thereby enabling a good visualization of change in frequency content over time (Park, 2009). Additionally, in order to quantify the variations in average power content of the frequencies present in the hemodynamic signals through different phases of anesthesia, their power spectral density (periodogram from MATLAB, window type = hamming, window length = length of the signal, sampling points (nfft) = next power of 2 which is greater than the length of the signal duration) was also calculated independently for each anesthetic phase of interest. The integrated average power estimates for every anesthetic phase within specific frequency bands (0.1 Hz – 0.5 Hz band and 0.01 Hz – 0.10 Hz band) were also calculated (MATLAB bandpower).

For further analysis, the cerebral hemodynamic signals were band-pass filtered (order = 20, design method = Kaiser window FIR filter) between 0.01 and 0.10 Hz to focus on the low-frequency oscillations (LFO). To explore the variations in cerebral hemodynamic signals, through the different phases of anesthesia, two other parameters were calculated for every anesthetic phase of interest – (i) Sample Entropy (a measure of complexity) and (ii) the phase difference between Δ[HbO] and Δ[Hb]...

Sample entropy: The sample entropy is defined as the negative natural logarithm of the conditional probability that two sequences similar for 'm' points, remain similar at the next point, with the exclusion of self matches. It is used as a measure of similarity within time-series data. The algorithm is a modification of the approximate entropy algorithm, independent of data length, and exhibits better consistency than approximate entropy (Richman et al., 2011). In this study, the sample entropy of cerebral hemodynamic signals was calculated for every anesthetic phase using the MATLAB function SampEn.m (Monge-Álvarez, 2020). An embedding dimension of 2 and a tolerance of 0.2 times the standard deviation of the data was used based on previous suggestions (Perpetuini et al., 2019; Richman et al., 2011; Yentes et al., 2013).

Phase difference: Pierro et al. has demonstrated that the phase difference between Δ[HbO] and Δ[Hb] has the potential to unmask the hemodynamic mechanisms of cerebral physiology, activation, and pathological conditions (Pierro et al., 2012). The phase difference between Δ[HbO] and Δ[Hb] was calculated as the difference between the instantaneous phases of the respective signals, calculated by Hilbert's transform (Liang et al., 2018), and then projected in the range of [0 π] for every anesthetic phase for each patient.

2.4.2. EEG

The EEG signals were processed using MATLAB (MATLAB 2015b, The MathWorks Inc., Natick, MA, 2000) and Chronux toolbox (version 2.12; http://chronux.org/). The EEG signals from every channel of each patient were filtered in the range of 0.1 – 45 Hz (order = 20, design method = Kaiser window FIR filter) to remove the baseline drift and high frequency noise. Data from each channel was also denoised using a stationary wavelet transform based technique to remove the ocular artifacts from eye movements, as suggested previously (Krishnaveni et al., 2006). The signals from the two channels of EEG exhibited a very high correlation of 0.69 ± 0.19. All further analyses were hence carried out after averaging the responses from the two EEG channels for each subject to increase the signal–noise-ratio.

The Chronux toolbox was used to perform time–frequency analysis of the EEG signals in the range of 0.1 – 45 Hz, at a window length of 2 seconds and a 95 percent overlap.

EEG Entropy measures: For every anesthetic phase, the sample entropy and permutation entropy of EEG signals across the wide frequency range of 0.1 – 45 Hz were calculated using in-house entropy algorithms. An embedding dimension of 2 and a tolerance of 0.15 were used in sample entropy calculation, while an embedding dimension of 6 and a lag of 1 were used in permutation entropy calculation, as per previous suggestions (Li et al., 2008; Liang et al., 2015). In addition, sample entropy – across the six different sub frequency bands – were also calculated. More specifically, the bands were slow waves (0.1 – 1 Hz), delta (0.5 – 3 Hz), theta (3 – 8 Hz), alpha (8 – 12 Hz), beta (12 – 38 Hz) and gamma (38 – 42 Hz).

EEG Phase Difference: In case of fNIRS, the phase difference was calculated between two temporal series, oxy- and deoxyhemoglobin concentration changes, measured at the same region. However, in case of EEG, there is only one signal. Thus, phase calculation cannot be applied here.

2.4.3. Time - amplitude analysis of simultaneous fNIRS and EEG

To test the hypothesis that the hemodynamic signals could reflect the changes in neuronal activity, the fNIRS signals were filtered for low frequency oscillations (0.01 – 0.1 Hz) in small sliding windows, with no overlap. The length of the processing windows was empirically decided to be ~ 5 times the sampling frequency of the signal. The EEG signals were filtered in the range of 0.1 – 45 Hz in windows of length similar to its corresponding fNIRS window length. Similarity between the patterns of variation of these signals were examined through the cross correlation between standard deviations of both the signals in the corresponding processing windows.

2.4.4. Statistical analysis

Kruskal Wallis tests were used to determine statistically significant differences in average power estimates of fNIRS signals and average entropy values of fNIRS and EEG signals, between the different anesthetic phases. In addition, cluster-based permutation tests were used to determine statistically significant differences in average power of alpha range oscillations in the EEG signals, between the different anesthetic phases and age groups (Maris and Oostenveld, 2007).

3. Results

3.1. Time-Amplitude analysis

Fig. 3a and 3b respectively illustrate the time – course of fNIRS and EEG signal amplitudes of patient 23 (18 – 60 years group) and patient 1 (6–10 years group). It can be observed that the envelope of amplitude variation of cerebral hemodynamic signals very closely follows the pattern of variation in neuronal activity measured by EEG. Notably, this pattern is more visible in the older age group throughout the entire course of anesthesia as compared to the minor age group.

The correlation between amplitude changes in hemodynamic signals and neuronal signals exhibited by the older age group (Δ[HbO]: 0.44 ± 0.07, Δ[Hb]: 0.40 ± 0.10) is notably higher than that exhibited by the minor group (Δ[HbO]: 0.15 ± 0.02, Δ[Hb]: 0.10 ± 0.06). The results of correlation indices of similarity between the patterns of variation in hemodynamic and neuronal signals for all patients are summarized in Figure S1 (See Supplementary Material).

3.2. Time-frequency analysis

The spectrograms of fNIRS and EEG signals of patient 23 (18 – 60 years group) and patient 1 (6–10 years group) are depicted in Fig. 4a and 4b respectively. The spectrogram of Δ[HbO] and Δ[Hb] exhibits the presence of a ~0.2 Hz band (with less power in the age group of 6–10 years), during the anesthesia maintenance phase. This is attributed to the mechanically aided breathing during the surgical procedure. More importantly, there is a general decrease in the power of the spectrum during the maintenance phase among both groups. Fig. 5 summarizes this significant decrease in the average power of the cerebral hemodynamic signals during anesthesia maintenance compared to the baseline and post recovery, specifically in the frequency bands of 0.01 Hz – 0.1 Hz and 0.1 Hz – 0.5 Hz.

The spectral analysis of EEG shows the presence of slow waves (<1 Hz) throughout anesthesia and alpha range oscillations (~10 Hz) during the anesthesia maintenance phase in both age groups (see Figure S3). However, the 10 Hz frequency band appears to demarcate the loss and return of consciousness with a higher power in the age group of 6–10 years than in the older adults (See Figures S2 and S4 in the Supplementary Material). Also, the majority of the subjects in the minor group manifest this frequency band at the beginning of the recovery phase after the cessation of drug infusion, whereas among the adults, this band is present at a relatively lower power. See Figure S2 in the Supplementary Material for EEG results averaged over all the subjects.

3.3. Complexity of fNIRS and EEG

The sample entropies of Δ[HbO] and Δ[Hb] during the different anesthetic phases among the two different age groups are shown in Fig. 6a and 6b respectively. These results show that the anesthe-

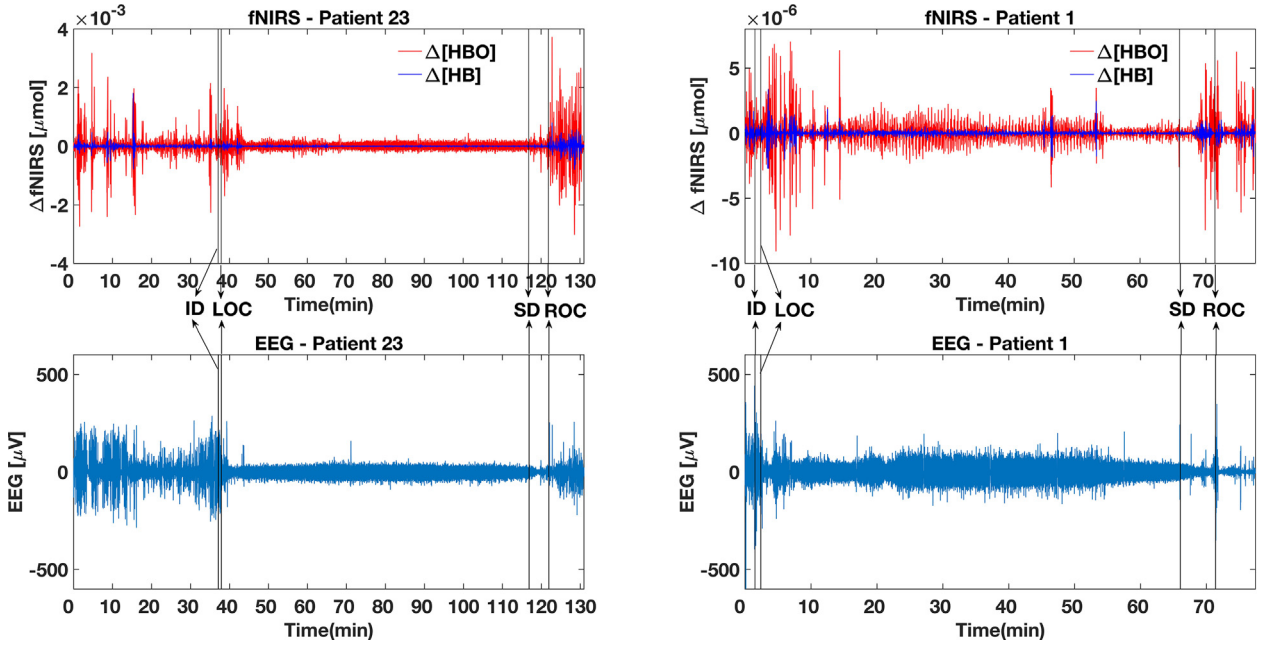

Fig. 3. Time course of fNIRS and EEG signal amplitudes of a) patient 23 (18 – 60 years group) and b) patient 1 (6–10 years group). fNIRS – functional Near Infrared Spectroscopy; Δ[HbO] – change in concentration of oxyhemoglobin; Δ[Hb] – change in concentration of deoxyhemoglobin; EEG – Electroencephalogram; ID – Infuse Drug; LOC – Loss of Consciousness; SD – Stop Drug; ROC – Recovery of Consciousness.

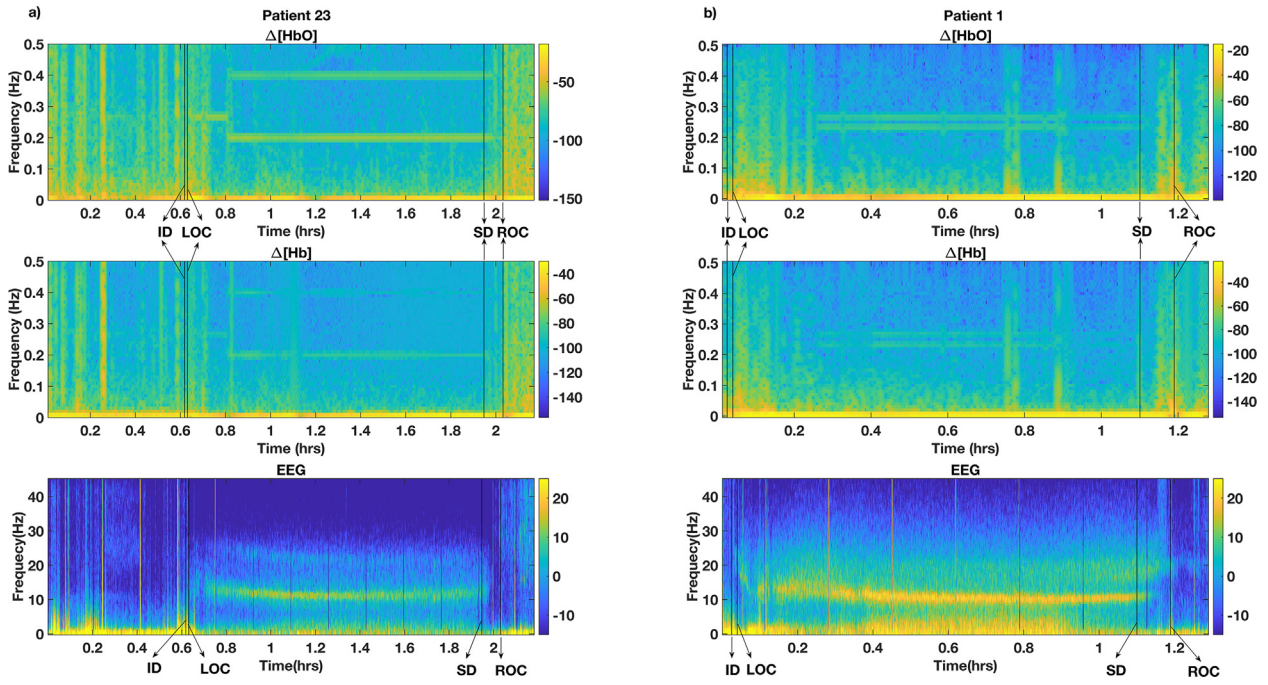

Fig. 4. Time – frequency analysis of fNIRS and EEG signals of a) patient 23 (18 – 60 years group) and b) patient 1 (6–10 years group). fNIRS – functional Near Infrared Spectroscopy; Δ[HbO] – change in concentration of oxyhemoglobin; Δ[Hb] – change in concentration of deoxyhemoglobin; EEG – Electroencephalogram; ID – Infuse Drug; LOC – Loss of Consciousness; SD – Stop Drug; ROC – Recovery of Consciousness.

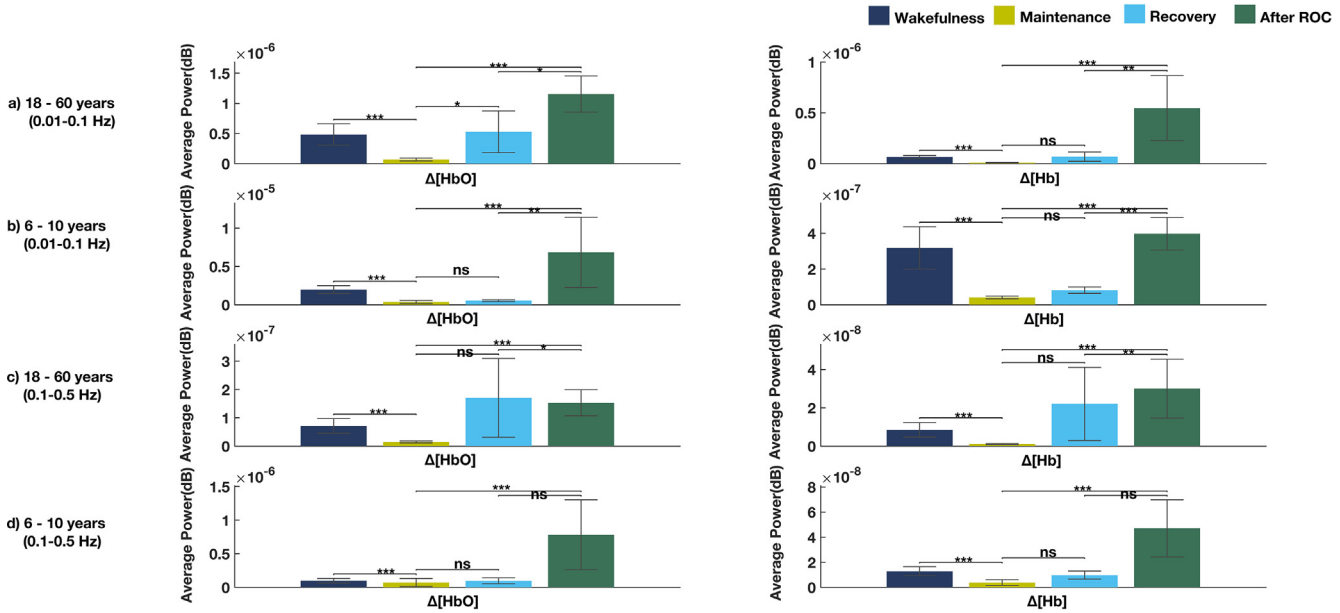

Fig. 5. Average Power of fNIRS signals through the different phases of anesthesia in a)18–60 years group in the frequency range of 0.01 Hz – 0.1 Hz, b) 6–10 years group, in the frequency range of 0.01 Hz – 0.1 Hz, c) 18 – 60 years group in the frequency range of 0.1 Hz – 0.5 Hz, and d) 6–10 years group in the frequency range of 0.1 Hz – 0.5 Hz. * ($p < 0.05$); ** ($p < 0.01$); *** ($p < 0.001$); **** ($p < 0.0001$). Δ[HbO] – change in concentration of oxyhemoglobin; Δ[Hb] – change in concentration of deoxyhemoglobin; ROC – Recovery of Consciousness.

sia maintenance phase is marked by a significantly lower sample entropy compared to wakefulness before anesthesia and the recovery phases. This also means that there is a significantly higher degree of similarity in the signals in the deep anesthesia phase and they are more dissimilar or more varied during wakefulness and recovery phases. Both the age groups exhibit the same pattern.

Fig. 6c illustrates the sample entropy of EEG (0.1 – 45 Hz) during the different anesthetic phases among the two different age groups. The results of sample entropy changes across the different sub frequency bands of EEG can be found in Figure S5 in the Supplementary Material. From these figures, it can be seen that the EEG sample entropy increases during the maintenance phase of anesthesia (unlike fNIRS). On the other hand, the complexity of EEG signals, characterized by permutation entropy (Fig. 6d), decreases significantly during the maintenance phase of anesthesia in both age groups. However, both EEG entropy measures were not

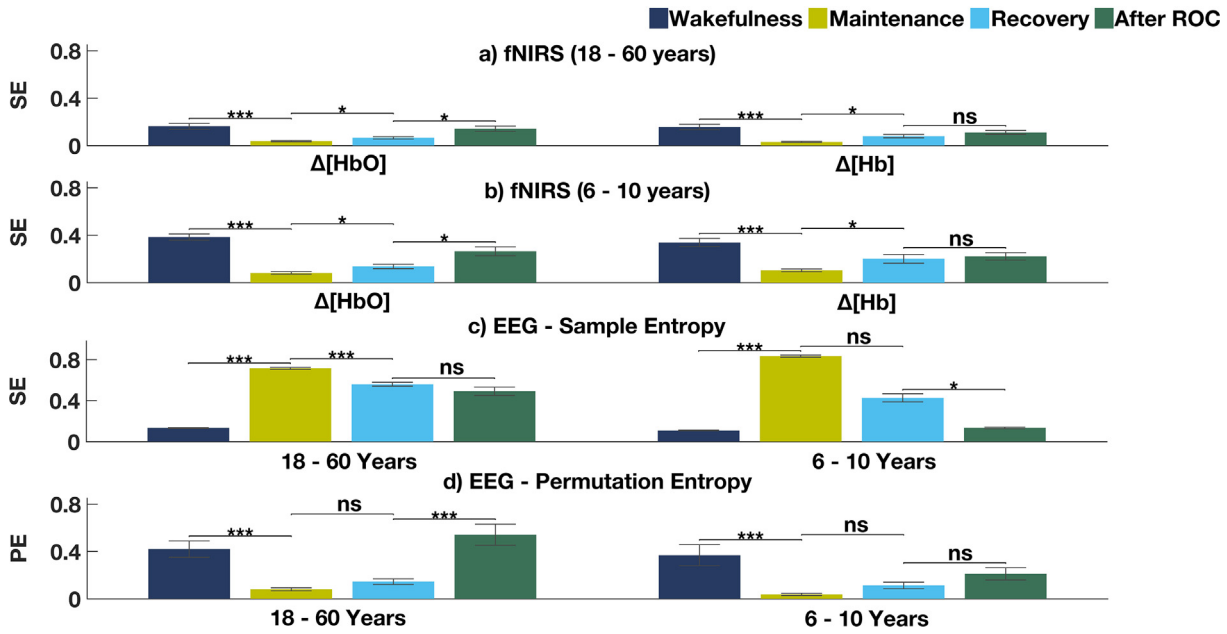

Fig. 6. Variation in sample entropy of fNIRS signals through the different phases of anesthesia in a) 18 – 60 years group and b) 6–10 years group and of (c) EEG signals (0.1 – 45 Hz) in both age groups. d) Variation in permutation entropy of EEG signals (0.1 – 45 Hz) through the different phases of anesthesia in both age groups. * ($p < 0.05$); ** ($p < 0.01$); ***($p < 0.001$); ****($p < 0.0001$). SE – Sample Entropy; PE – Permutation Entropy; fNIRS – functional Near Infrared Spectroscopy; EEG – Electroencephalogram; Δ[HbO] – change in concentration of oxyhemoglobin; Δ[Hb] – change in concentration of deoxyhemoglobin; ROC – Recovery of Consciousness.

as effective as fNIRS (i.e., Δ[HbO]) in isolating various anesthesia phases, in these two age groups.

3.4. Phase difference between Δ[HbO] and Δ[Hb]

The changes in the phase difference between Δ[HbO] and Δ[Hb] during the different anesthetic phases between the two different age groups are depicted in Fig. 7. It can be seen that in the age group of 18–60 years, during the phases before loss of consciousness, the majority of the subjects have a phase difference of around π, with a few outliers. However, during the deep anesthesia/maintenance phase, the phase differences are more spread out with most of them in the range of [2 π]. The scatter of phase differences increases even further during the recovery and post recovery phases. In the age group of 6–10 years, the same pattern as in the older age group could be observed until the maintenance phase of anesthesia, but the scatter tends to remain almost the same during the recovery phase and seems to return to baseline patterns after recovery. However, no significant changes between anesthetic phases were identified in either of the age groups.

4. Discussion

This study explores the distinct signatures of general anesthesia in neural and hemodynamic responses and their underlying physiological mechanisms based on simultaneously acquired fNIRS and EEG. The findings illustrate reliable differences in parameters measured from hemodynamic and neuronal activities between different anesthetic phases as well as between the studied age groups. Identification of unique biomarkers in different anesthetic phases from the cerebral hemodynamic signals could not only help unveil the precise mechanisms of anesthesia, but also help develop an efficient anesthesia depth monitor when paired with established EEG signatures.

4.1. Power changes of fNIRS

Fig. 3 shows the correlations between the magnitude changes of EEG and fNIRS signals. The decrease in neural activity induced by the anesthetic agents was observed in the EEG signal as a decrease in the magnitude of the signal during the maintenance phase. Since the fNIRS signal is influenced by very low frequency components (<0.01 Hz), we used a sliding window to remove these influences. The results of this analysis demonstrated that fNIRS can reflect this underlying neuronal activity by showing a similar trend in the magnitude changes in hemodynamic signals. Lower signal magnitude in fNIRS might reflect reduced metabolic demand and low regional cerebral blood flow induced by propofol (Conti et al., 2006) and by sevoflurane (Palanca et al., 2017).

To further quantify the power distribution in different anesthetic phases, we plotted the time–frequency analysis of the signals (Fig. 4) using spectrograms and average power estimates (Fig. 5). First of all, the time–frequency analysis of EEG signals illustrates both the coherent frontal alpha oscillations (~10 Hz), referred to as anteriorization of the alpha rhythm, and slow waves (<1 Hz), a well – established EEG signature of sevoflurane and propofol (Akeju et al., 2014) (Fig. 4 and Figure S2). A plethora of research has explained that these highly organized coherent alpha oscillations presumably block the communication or coupling between the thalamus and cortex, whereas the incoherent slow oscillations restrict the normal intracortical communications (Akeju et al., 2014; Hagihira, 2015; Hight et al., 2017; Lewis et al., 2012; Mhuircheartaigh et al., 2013; Purdon et al., 2013). It has also been suggested that these alpha oscillations predominate when the anesthesia is adequate for surgery (Hagihira, 2015). Compared to alpha oscillations, we can see a 0.2 Hz oscillation in fNIRS throughout the period from loss of consciousness to recovery of consciousness. However, this frequency and its harmonics were caused by forced breathing (~0.2 Hz) during the surgery. Thus, there is no corresponding "signature signal", as with alpha range oscillations in EEG, in fNIRS. Secondly, the power of the fNIRS signal over a wide frequency range during the maintenance phase is significantly lower compared to the baseline and post recovery.

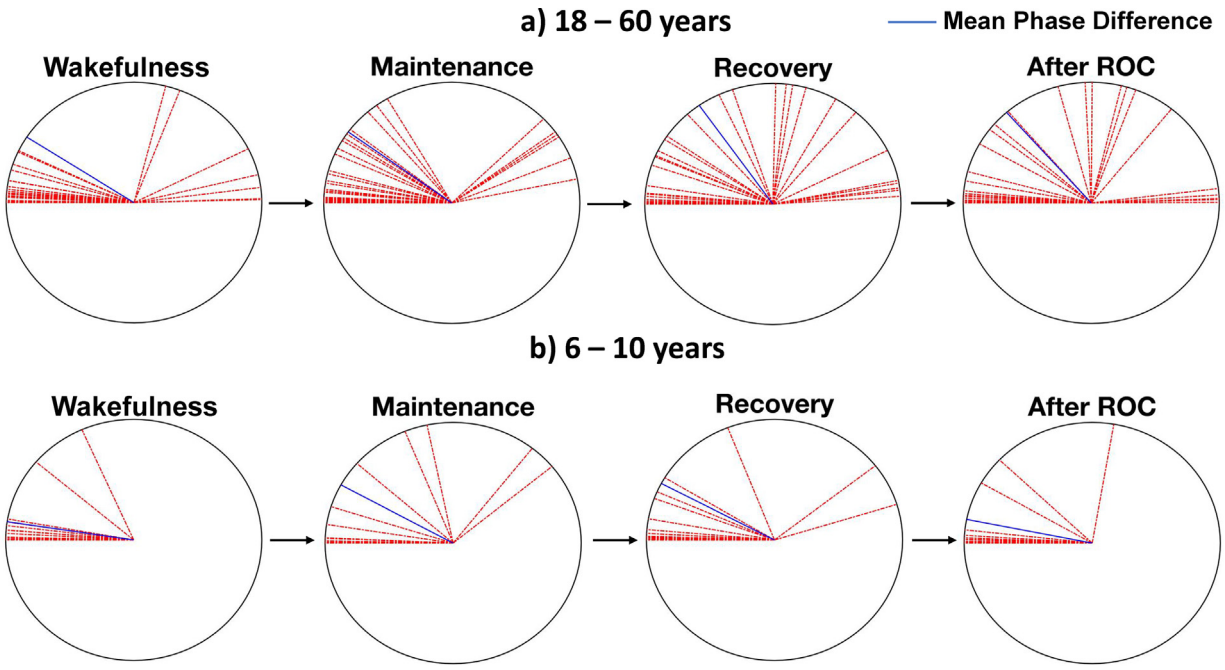

Fig. 7. Variation in phase difference between Δ[HbO] and Δ[Hb] through the different phases of anesthesia in a) 18 – 60 years group and b) 6–10 years group. Δ[HbO] – change in concentration of oxyhemoglobin; Δ[Hb] – change in concentration of deoxyhemoglobin; ROC – Recovery of Consciousness.

This can also be seen in the spectrogram as color, representing power, shifted towards blue in the same period. Since fNIRS measures neuronal activities through neurovascular coupling (i.e., equivalent to low-pass filter), the frequency band that is associated with neuronal activation is below 0.1 Hz. The signals with higher frequencies (>0.1 Hz) are thought to be associated with physiological processes, such as breathing, heartbeat, etc. In this study, we can see that the power drop happened in both frequency bands during the maintenance phase. The power reduction in the low frequency band is consistent with previous findings from BOLD fMRI signals during propofol and sevoflurane anesthesia (Zhang et al., 2018). Thirdly, the power drop period is generally shorter than the duration from loss of consciousness to recovery of consciousness (Fig. 4). This might indicate the power change is a slow process, which does not happen instantaneously with the injection/withdrawal of the drug. This can also be seen in Fig. 5, where the recovery phase only shows a relative increase in power in both the higher frequency and low frequency oscillation bands, and a significant change is only observed after recovery of consciousness.

4.2. Sample entropy

Another important finding from the present study is about the sample entropy of fNIRS signals. Different from the power, sample entropy reflects the degree of signal's regularity. It was found that the sample entropy of cerebral hemodynamic signals (0.01 Hz – 0.1 Hz), observed during the anesthesia maintenance phase, is significantly lower as compared to the phases before the loss of consciousness and the recovery phase. Besides Fig. 6, Fig. 4 also showed the variations in the low frequency range (<0.1 Hz, neuronal signal) decreased in the maintenance phase (i.e., the color became more uniform in the spectrogram). This is likely caused by the potent cerebral metabolic suppression induced by propofol (Oshima et al., 2002) and maintained with sevoflurane (Kaisti et al., 2003). A robustly reduced global cerebral blood flow state by sevoflurane (up to concentrations of 4 percent) was found in other studies (Kaisti et al., 2002), which might also explain this effect. It is worth noting that the forced breathing (~0.2 Hz) in the maintenance phase has also contributed to the regularity of the signal (Fig. 4), further decreasing the entropy.

In contrast, once the drug started to wash out from the system, more variations in the cerebral hemodynamic signals appeared, as indicated by a significantly higher sample entropy during the recovery phase. In a similar line, Izzetoglu et al. reported that the rate of Δ[Hb] and total hemoglobin is significantly lower during the anesthesia maintenance phase as compared to significantly larger rates of changes during the recovery phase and that this difference could be used as a reliable marker to distinguish maintenance and recovery phases (Izzetoglu, 2008). Interestingly, the value of sample entropy in the recovery phase was still significantly lower than that of the baseline, indicating the residual effect of the drug. The observation is very different from that of the power (Fig. 5), where the power in the recovery phase is relatively higher than that of baseline, among the adult population, in both frequency bands. This might indicate the different underlying mechanisms represented by power and entropy, in which one overcompensates in the recovery phase, while the other undercompensates.

Along similar lines, significant decreases in different EEG entropy measures (Liang et al., 2015) during sevoflurane anesthesia and EEG complexity during propofol and Ketamine anesthesia (Schartner et al., 2015; Wang et al., 2017), and subsequent increases during recovery have been reported. We have found a similar result using permutation entropy (Li et al., 2008; Liang et al., 2015) (Fig. 6d). However, results using sample entropy showed increases in the complexity of EEG during the maintenance phase of anesthesia (Fig. 6c). Sample entropy quantifies the complexity of a time series on a limited scale (Liu et al., 2015), which is why it is well-suited to fNIRS data with a narrow frequency band (0.01–0.1 Hz). However, EEG is an integrated signal of cortical activity that is controlled by complex self-regulating and interacting systems running across multiple time scales (Shalbaf et al., 2014). It might be more effective to apply sample entropy on specific frequency bands, instead of the signal with full spectrum. In addition, EEG sample entropy was reported to be less reliable compared to other entropy measures, possibly due to its high sensitivity to noise (Liang et al., 2015). Lastly, there could also be

differences in the complexity of EEG signals arising from different brain regions during anesthesia (Liu et al., 2018) and factors such as pre-operative anxiety during wakefulness might reduce the EEG sample entropy during this period (Tran et al., 2007). However, these interesting questions about various EEG entropy measures are beyond the scope of this manuscript. We will try to address them in the future studies with more data.

Finally, Wang et al. has reported a significantly higher sample entropy of fNIRS signals during the propofol anesthesia maintenance phase, when compared to waking phases (Wang et al., 2020). These results could have been due to the short lengths of the post-operative waking phases, leading to inadequate analysis window lengths in those phases (Richman et al., 2011; Yentes et al., 2013).

4.3. Phase difference between Δ[HbO] and Δ[Hb]

Analysis of phase differences between Δ[HbO] and Δ[Hb] during the different anesthetic phases among both age groups did not reveal significant changes, indicating that phase difference might not have enough sensitivity to distinguish the status of the anesthesia. A previous study found that phase difference was closely related to the early development of brain (Watanabe et al., 2017). It becomes stable (i.e. phase$\approx\pi$) for babies older than 3 months (Taga et al., 2017) and it does not change until old age (>65) (Liang et al., 2018). This observation suggested that phase difference represented some robust underlying physiology/vasculature, which does not change easily after development. In this study, we found that even anesthetic drugs cannot make significant changes to the phase difference. This observation confirmed that the underlying physiological condition represented by the phase difference is so crucial and basic to life, it forms very early on in the child development and hardly changes under the influence of other potent factors.

4.4. Children versus adults

The differences in both EEG and fNIRS signals depending on the age were observed in this study. For example, the adults exhibited a higher degree of correlation between the neuronal and vascular responses (signal magnitude), whereas the children's correlation values were much lower (Figure S1). Since general anesthesia has been reported to affect the neurovascular coupling process (Masamoto and Kanno, 2012), one possible explanation for this observation could be that neurovascular coupling is still immature in the developing brain (Kozberg and Hillman, 2016). Mounting evidence also suggests varied responses in cerebral blood flow to sensory stimulation in children when compared to adults (Born et al., 2002; Moses et al., 2014).

Furthermore, previous studies have shown that the EEG oscillations during anesthesia differ significantly in children as compared to adults (Davidson et al., 2008; Lo et al., 2009). In our study, it could also be discerned from Figure S2, that the changes in EEG power throughout the different anesthetic phases vary between the age groups. For example, frontal EEG alpha power is higher in children compared to adults (Figures S2 and S4). The fact that the alpha – range oscillations continued to be present in the recovery phase with a relatively higher power in minors, would translate into a more varied process in the developing brain to reestablish the higher-order connections blocked by the drug. In view of the thalamocortical development that occurs throughout childhood, Lee et al. has reported age-related changes in EEG alpha power and coherence during propofol anesthesia and suggests that a more specific and principled approach to monitoring brain states is needed for pediatric patients (Lee et al., 2017). Increased frontal EEG alpha power during sevoflurane anesthesia has also been reported in infants of 4 – 6 months of age, with suggestions about differences in developmental factors such as synaptogenesis, glucose metabolism and myelination across cortex likely contributing to the observed effect (Cornelissen et al., 2015). Moreover, the fading of alpha – range oscillations towards the end of the recovery phase in children, indicates that this process is faster in children than adults. This could be attributed to relatively faster washout of sevoflurane due to its low solubility in blood and tissues (Sarner et al., 1995) combined with shorter elimination half-lives and higher plasma clearance for propofol (Maheshwari et al., 2019; Murat et al., 1996). All contribute to a faster emergence from anesthesia in children when compared to adults.

These observations, together with the fact that neural circuits undergo significant developmental changes from birth to adulthood (Tau and Peterson, 2010), suggest that when monitoring brain states under general anesthesia, one must consider the patient's age.

4.5. Importance of a multimodal approach

The power differences in the frontal EEG alpha range oscillations between the studied age groups which are present throughout the time from loss of consciousness to recovery of consciousness (Figure S2), makes this signal an important marker of the effect of age in measuring anesthesia depth. However, the fact that it disappears only after a patient recovers consciousness (in both age groups) does not give a sufficient lead time to take any actions in the event of a reduced anesthesia depth during the surgery, and hence, might not be able to prevent intra-operative awareness. However, a significant increase in sample entropy and a relative increase in power of fNIRS signals could be observed during the recovery phase as compared to the maintenance phase, even before the patients completely recover consciousness. These measures therefore are important with respect to predicting emergence from general anesthesia with a sufficient lead time to prevent intra-operative awareness. Thus, a multimodal approach based on both fNIRS and EEG comprehensively addresses all the requirements of brain state monitoring during the complete general anesthesia process.

4.6. Limitations

The results from this study are limited to the neurovascular responses from the pre-frontal cortex. Moreover, this study only characterized the general anesthesia induced by propofol and maintained with sevoflurane. It would be interesting to compare the effects of different anesthetic agents using simultaneous fNIRS and EEG. Future research should focus on the development of an anesthesia depth index based on both fNIRS and EEG, incorporating an analysis of spatial variations in neurovascular responses and their differences across age groups.

5. Conclusion

The results of this study illustrate that the phases of general anesthesia can be characterized from fNIRS signals. We have shown that fNIRS can reliably reflect underlying neuronal activity during the complete general anesthesia process in the adult population. Significant changes in the complexity and power of fNIRS signals also differentiate the different anesthetic phases among adults and children. This, therefore, leads us to conclude that fNIRS can offer complementary neurovascular assessment on general anesthesia, which can greatly improve the accuracy when combined with EEG measurement. Furthermore, the differences in neurovascular coupling and neural activity under anesthesia between

adults and children, as illustrated in this study, might also be taken under serious consideration.

Declaration of Competing Interest

The authors declare that they have no known competing financial interests or personal relationships that could have appeared to influence the work reported in this paper.

Acknowledgements

This research was supported by the National Natural Science Foundation of China (61673333), Natural Science Fund for Excellent Young Scholars of Hebei Province of China (F2018203281). The sponsors were not involved in the collection, analysis and interpretation of data and in the writing of the manuscript.

Appendix A. Supplementary data

Supplementary data to this article can be found online at https://doi.org/10.1016/j.clinph.2021.03.025.

References

Akeju O, Westover MB, Pavone KJ, Sampson AL, Hartnack KE, Brown EN, et al. Effects of sevoflurane and propofol on frontal electroencephalogram power and coherence. Anesthesiol J Am Soc Anesthesiol 2014;121:990–8.

Avidan MS, Jacobsohn E, Glick D, Burnside BA, Zhang L, Villafranca A, et al. Prevention of intraoperative awareness in a high-risk surgical population. N Engl J Med 2011;365:591–600.

Avidan MS, Mashour GA. The incidence of intraoperative awareness in the UK: Under the rate or under the radar?. Br J Anaesth 2013;110:494–7. https://doi.org/10.1093/bja/aet012.

Bischoff P, Rundshagen I. Awareness Under General Anesthesia. Dtsch Arztebl 2011;108:1–7. https://doi.org/10.3238/arztebl.2011.0001.

Boas DA, Elwell CE, Ferrari M, Taga G. Celebrating 20 Years of Functional Near Infrared Spectroscopy (fNIRS). NeuroImage (Orlando. Fla) 2014;85.

Born AP, Rostrup E, Miranda MJ, Larsson HBW, Lou HC. Visual cortex reactivity in sedated children examined with perfusion MRI (FAIR). Magn Reson Imaging 2002;20:199–205. https://doi.org/10.1016/S0730-725X(02)00469-1.

Brown EN, Lydic R, Schiff ND. General anesthesia, sleep, and coma. N Engl J Med 2010;363:2638–50. https://doi.org/10.1056/NEJMra0808281.

Brown EN, Pavone KJ, Naranjo M. Multimodal general anesthesia: Theory and practice. Anesth Analg 2018;127:1246–58. https://doi.org/10.1213/ANE.0000000000003668.

Bruhn J, Myles PS, Sneyd R, Struys MMRF. Depth of anaesthesia monitoring: What's available, what's validated and what's next?. Br J Anaesth 2006;97:85–94. https://doi.org/10.1093/bja/ael120.

Conti A, Iacopino DG, Fodale V, Micalizzi S, Penna O, Santamaria LB. Cerebral haemodynamic changes during propofol-remifentanil or sevoflurane anaesthesia: Transcranial Doppler study under bispectral index monitoring. Br J Anaesth 2006;97:333–9. https://doi.org/10.1093/bja/ael169.

Cornelissen L, Kim S, Purdon PL, Brown EN, Berde CB. Age-dependent electroencephalogram (EEG) patterns during sevoflurane general anesthesia in infants 2015:1–25. https://doi.org/10.7554/eLife.06513.

Cui X, Bray S, Reiss AL. Functional near infrared spectroscopy (NIRS) signal improvement based on negative correlation between oxygenated and deoxygenated hemoglobin dynamics. Neuroimage 2010;49:3039–46. https://doi.org/10.1016/j.neuroimage.2009.11.050.

Davidson AJ, Sale SM, Wong C, Mckeever S, Sheppard S, Chan Z, et al. The electroencephalograph during anesthesia and emergence in infants and children. Paediatr Anaesth 2008;18:60–70. https://doi.org/10.1111/j.1460-9592.2007.02359.x.

Ferrari M, Quaresima V. A brief review on the history of human functional near-infrared spectroscopy (fNIRS) development and fields of application. Neuroimage 2012;63:921–35.

Franks NP. General anaesthesia: from molecular targets to neuronal pathways of sleep and arousal. Nat Rev Neurosci 2008;9:370–86.

Giraldo J, Acosta C, Giraldo-Grueso M. Frequency of anesthetic overdose with mean alveolar concentration-guided anesthesia at high altitude. Med Gas Res 2018;8:150–3. https://doi.org/10.4103/2045-9912.248265.

Hagihira S. Changes in the electroencephalogram during anaesthesia and their physiological basis. Br J Anaesth 2015;115:i27–31.

Hernandez-Meza G, Izzetoglu M, Osbakken M, Green M, Abubakar H, Izzetoglu K. Investigation of optical neuro-monitoring technique for detection of maintenance and emergence states during general anesthesia. J Clin Monit Comput 2018;32:147–63. https://doi.org/10.1007/s10877-017-9998-x.

Hernandez-Meza G, Izzetoglu M, Sacan A, Green M, Izzetoglu K. Investigation of data-driven optical neuromonitoring approach during general anesthesia with sevoflurane. Neurophotonics 2017;4:1. https://doi.org/10.1117/1.nph.4.4.041408.

Hight D, Voss LJ, Garcia PS, Sleigh J. Changes in alpha frequency and power of the electroencephalogram during volatile-based general anesthesia. Front Syst Neurosci 2017;11:36.

Ishioka Y, Sugino S, Hayase T, Janicki PK. Intraoperative auditory evoked potential recordings are more reliable at signal detection from different sensor sites on the forehead compared to bispectral index. J Clin Monit Comput 2017;31:117–22. https://doi.org/10.1007/s10877-015-9812-6.

Izzetoglu K and Onaral B, "Neural correlates of cognitive workload and anesthetic depth: fNIR spectroscopy investigation in humans," PhD Thesis Drexel University, Philadelphia, PA, 2008.

Izzetoglu K, Ayaz H, Merzagora A, Izzetoglu M, Shewokis PA, Bunce SC, et al. The evolution of field deployable FNIR Spectroscopy from bench to clinical settings. J Innov Opt Health Sci 2011;4:239–50.

Kaisti KK, Långsjö JW, Aalto S, Oikonen V, Sipilä H, Teräs M, et al. Effects of sevoflurane, propofol, and adjunct nitrous oxide on regional cerebral blood flow, oxygen consumption and blood volume in humans. Anesthesiology 2003;99:603–13. https://doi.org/10.1097/00000542-200309000-00015.

Kaisti KK, Metsähonkala L, Teräs M, Oikonen V, Aalto S, Jääskeläinen S, et al. Effects of surgical levels of propofol and sevoflurane anesthesia on cerebral blood flow in healthy subjects studied with positron emission tomography. Anesthesiology 2002;96:1358–70. https://doi.org/10.1097/00000542-200206000-00015.

Kent CD, Mashour GA, Metzger NA, Posner KL, Domino KB. Psychological impact of unexpected explicit recall of events occurring during surgery performed under sedation, regional anaesthesia, and general anaesthesia: Data from the Anesthesia Awareness Registry. Br J Anaesth 2013;110:381–7. https://doi.org/10.1093/bja/aes386.

Khan MS, Zetterlund EL, Gréen H, Oscarsson A, Zackrisson AL, Svanborg E, et al. Pharmacogenetics, Plasma Concentrations, Clinical Signs and EEG During Propofol Treatment. Basic Clin Pharmacol Toxicol 2014;115:565–70. https://doi.org/10.1111/bcpt.12277.

Kozberg M, Hillman E. Neurovascular coupling and energy metabolism in the developing brain. Prog Brain Res 2016;225:213–42. https://doi.org/10.1016/bs.pbr.2016.02.002.

Krishnaveni V, Jayaraman S, Anitha L, Ramadoss K. Removal of ocular artifacts from EEG using adaptive thresholding of wavelet coefficients. J Neural Eng 2006;3.;3. https://doi.org/10.1088/1741-2560/3/4/011.

Lee JM, Akeju O, Sc MM, Terzakis K, Pavone KJ, Shank ES, et al. Propofol-induced Electroencephalogram Oscillations. Anesthesiology 2017:293–306.

Leon-Dominguez U, Izzetoglu M, Leon-Carrion J, Solís-Marcos I, Garcia-Torrado FJ, Forastero-Rodríguez A, et al. Molecular concentration of deoxyHb in human prefrontal cortex predicts the emergence and suppression of consciousness. Neuroimage 2014;85:616–25. https://doi.org/10.1016/j.neuroimage.2013.07.023.

Leslie K, Myles PS, Forbes A, Chan MTV. The effect of bispectral index monitoring on long-term survival in the B-aware trial. Anesth Analg 2010;110:816–22. https://doi.org/10.1213/ANE.0b013e3181c3bfb2.

Leslie K, Myles PS, Forbes A, Chan MTV, Short TG, Swallow SK. Recovery from bispectral index-guided anaesthesia in a large randomized controlled trial of patients at high risk of awareness. Anaesth Intensive Care 2005;33:443–51. https://doi.org/10.1177/0310057x0503300404.

Lewis LD, Weiner VS, Mukamel EA, Donoghue JA, Eskandar EN, Madsen JR, et al. Rapid fragmentation of neuronal networks at the onset of propofol-induced unconsciousness. Proc Natl Acad Sci U S A 2012;109.;109. https://doi.org/10.1073/pnas.1210907109.

Li G, Warner M, Lang BH, Huang L, Sun LS. Epidemiology of anesthesia-related mortality in the United States, 1999–2005. Anesthesiol J Am Soc Anesthesiol 2009;110:759–65.

Li X, Cui S, Voss LJ. Using permutation entropy to measure the electroencephalographic effects of sevoflurane. Anesthesiology 2008;109:448–56. https://doi.org/10.1097/ALN.0b013e318182a91b.

Liang Z, Gu Y, Duan X, Cheng L, Liang S, Tong Y, et al. Design of multichannel functional near-infrared spectroscopy system with application to propofol and sevoflurane anesthesia monitoring. Neurophotonics 2016;3. https://doi.org/10.1117/1.nph.3.4.045001 045001.

Liang Z, Minagawa Y, Yang H-C, Tian H, Cheng L, Arimitsu T, et al. Symbolic time series analysis of fNIRS signals in brain development assessment. J Neural Eng 2018;15:66013. https://doi.org/10.1088/1741-2552/aae0c9.

Liang Z, Wang Y, Sun X, Li D, Voss LJ, Sleigh JW, et al. EEG entropy measures in anesthesia. Front Comput Neurosci 2015;9:1–17. https://doi.org/10.3389/fncom.2015.00016.

Liu Q, Chen YF, Fan SZ, Abbod MF, Shieh JS. EEG Signals Analysis Using Multiscale Entropy for Depth of Anesthesia Monitoring during Surgery through Artificial Neural Networks. Comput Math Methods Med 2015;2015.;2015. https://doi.org/10.1155/2015/232381.

Liu Q, Ma L, Fan SZ, Abbod MF, Shieh JS. Sample entropy analysis for the estimating depth of anaesthesia through human EEG signal at different levels of unconsciousness during surgeries. PeerJ 2018;2018:1–25. https://doi.org/10.7717/peerj.4817.

Lo SS, Sobol JB, Mallavaram N, Carson M, Chang C, Grieve PG, et al. Anesthetic-specific electroencephalographic patterns during emergence from sevoflurane and isoflurane in infants and children. Paediatr Anaesth 2009;19:1157–65. https://doi.org/10.1111/j.1460-9592.2009.03128.x.

Maheshwari M, Sanwatsarkar S, Katakwar M. Pharmacology related to paediatric anaesthesia. Indian J Anaesth 2019;63:698.
Manyam SC, Gupta DK, Johnson KB, White JL, Pace NL, Westenskow DR, et al. When is a bispectral index of 60 too low? Rational processed electroencephalographic targets are dependent on the sedative–opioid ratio. Anesthesiol J Am Soc Anesthesiol 2007;106:472–83.
Maris E, Oostenveld R. Nonparametric statistical testing of EEG- and MEG-data. J Neurosci Methods 2007;164:177–90. https://doi.org/10.1016/j.jneumeth.2007.03.024.
Masamoto K, Kanno I. Anesthesia and the quantitative evaluation of neurovascular coupling. J Cereb Blood Flow Metab 2012;32:1233–47. https://doi.org/10.1038/jcbfm.2012.50.
Mhuircheartaigh RN, Warnaby C, Rogers R, Jbabdi S, Tracey I. Slow-wave activity saturation and thalamocortical isolation during propofol anesthesia in humans. Sci Transl Med 2013;5:1–9. https://doi.org/10.1126/scitranslmed.3006007.
Monge-Álvarez J (2020). A set of Entropy measures for temporal series (1D signals) (https://www.mathworks.com/matlabcentral/fileexchange/50289-a-set-of-entropy-measures-for-temporal-series-1d-signals), MATLAB Central File Exchange. Retrieved December 24, 2020.
Moses P, Hernandez LM, Orient E. Age-related differences in cerebral blood flow underlie the BOLD fMRI signal in childhood. Front Psychol 2014;5:1–9. https://doi.org/10.3389/fpsyg.2014.00300.
Murat I, Billard V, Vernois J, Zaouter M, Marsol P, Souron R, et al. Pharmacokinetics of Propofol after a Single Dose in Children Aged 1–3 Years with Minor BurnsComparison of Three Data Analysis Approaches. Anesthesiol J Am Soc Anesthesiol 1996;84:526–32.
Naguib M, Samarkandi AH, Ammar A, Elfaqih SR, Al-Zahrani S, Turkistani A. Comparative clinical pharmacology of rocuronium, cisatracurium, and their combination. Anesthesiol J Am Soc Anesthesiol 1998;89:1116–24.
Oshima T, Karasawa F, Satoh T. Effects of propofol on cerebral blood flow and the metabolic rate of oxygen in humans. Acta Anaesthesiol Scand 2002;46:831–5. https://doi.org/10.1034/j.1399-6576.2002.460713.x.
Oxorn DC, Ferris LE, Harrington E, Orser BA. The effects of midazolam on propofol-induced anesthesia: Propofol dos requirements, mood profiles, and perioperative dreams. Anesth Analg 1997;85:553–9. https://doi.org/10.1097/00000539-199709000-00013.
Palanca BJA, Avidan MS, Mashour GA. Human neural correlates of sevoflurane-induced unconsciousness. BJA 2017;119:573–82. https://doi.org/10.1093/bja/aex244.
Park TH. Introduction to digital signal processing: Computer musically speaking. World Scientific; 2009.
Perpetuini D, Chiarelli AM, Cardone D, Filippini C, Bucco R, Zito M, et al. Complexity of frontal cortex fNIRS can support Alzheimer disease diagnosis in memory and visuo-spatial tests. Entropy 2019;21.;21. https://doi.org/10.3390/e21010026.
Pierro ML, Sassaroli A, Bergethon PR, Ehrenberg BL, Fantini S. Phase-amplitude investigation of spontaneous low-frequency oscillations of cerebral hemodynamics with near-infrared spectroscopy: a sleep study in human subjects. Neuroimage 2012;63:1571–84.
Purdon PL, Pierce ET, Mukamel EA, Prerau MJ, Walsh JL, Wong KFK, et al. Electroencephalogram signatures of loss and recovery of consciousness from propofol. Proc Natl Acad Sci U S A 2013;110.;110. https://doi.org/10.1073/pnas.1221180110.
Purdon PL, Sampson A, Pavone KJ, Brown EN. Clinical electroencephalography for anesthesiologistspart I: background and basic signatures. Anesthesiol J Am Soc Anesthesiol 2015;123:937–60.
Reves JG, Fragen RJ, Vinik HR, Greenblatt DJ. Midazolam: pharmacology and uses. Anesthesiology 1985;62:310–24.
Richman JS, Moorman JR, Gilmour TP, Piallat B, Lieu CA, Venkiteswaran K, et al. Physiological time-series analysis using approximate entropy and sample entropy Physiological time-series analysis using approximate entropy and sample entropy. Cardiovasc Res 2011;278:2039–49.
Rudolph U, Antkowiak B. Molecular and neuronal substrates for general anaesthetics. Nat Rev Neurosci 2004;5:709–20. https://doi.org/10.1038/nrn1496.
Sarner JB, Levine M, Davis PJ, Lerman J, Cook RD, Motoyama EK. Clinical characteristics of sevoflurane in children A comparison with halothane. Anesthesiol J Am Soc Anesthesiol 1995;82:38–46.
Schartner M, Seth A, Noirhomme Q, Boly M, Bruno MA, Laureys S, et al. Complexity of multi-dimensional spontaneous EEG decreases during propofol induced general anaesthesia. PLoS One 2015;10:1–21. https://doi.org/10.1371/journal.pone.0133532.
Sear JW. Recent advances and developments in the clinical use of i.v. opioids during the peroperative period. Br J Anaesth 1998;81:38–50.;81:38–50. https://doi.org/10.1093/bja/81.1.38.
Shalbaf R, Behnam H, Jelveh MH. Monitoring depth of anesthesia using combination of EEG measure and hemodynamic variables. Cogn Neurodyn 2014;9:41–51. https://doi.org/10.1007/s11571-014-9295-z.
Sinclair RCF, Faleiro RJ. Delayed recovery of consciousness after anaesthesia. Contin Educ Anaesthesia, Crit Care Pain 2006;6:114–8. https://doi.org/10.1093/bjaceaccp/mkl020.
Strawbridge AD, Khanna NR, Hauser JM. Cisatracurium. 2020 Jul 10. In: StatPearls [Internet]. Treasure Island (FL): StatPearls Publishing; 2021 Jan–. PMID: 30969664.
Taga G, Watanabe H, Homae F. Spatial variation in the hemoglobin phase of oxygenation and deoxygenation in the developing cortex of infants. Neurophotonics 2017;5:1. https://doi.org/10.1117/1.nph.5.1.011017.
Tau GZ, Peterson BS. Normal development of brain circuits. Neuropsychopharmacology 2010;35:147–68. https://doi.org/10.1038/npp.2009.115.
Tran Y, Thuraisingham RA, Wijesuriya N, Nguyen HT, Craig A. Detecting neural changes during stress and fatigue effectively: A comparison of spectral analysis and sample entropy. Proc 3rd Int IEEE EMBS Conf Neural Eng 2007:350–3. https://doi.org/10.1109/CNE.2007.369682.
Viertio-Oja H, Maja V, Sarkela M, Talja P, Tenkanen N, Tolvanen-Laakso H, et al. Description of the Entropytm algorithm as applied in the Datex-Ohmeda S/5 tm Entropy Module. Acta Anaesthesiol Scand 2004;48:154–61.
Wang G, Yan X, Liu Z, Feng Y, Jinming Li, Dong H, et al. Monitoring the Depth of Anesthesia through the Use of Cerebral Hemodynamic Measurements Based on Sample Entropy Algorithm. IEEE Trans Biomed Eng 2020;67:807–16.;67:807–16. https://doi.org/10.1109/TBME.2019.2921362.
Wang J, Noh GJ, Choi BM, Ku SW, Joo P, Jung WS, et al. Suppressed neural complexity during ketamine- and propofol-induced unconsciousness. Neurosci Lett 2017;653:320–5. https://doi.org/10.1016/j.neulet.2017.05.045.
Watanabe H, Shitara Y, Aoki Y, Inoue T, Tsuchida S, Takahashi N, et al. Hemoglobin phase of oxygenation and deoxygenation in early brain development measured using fNIRS. Proc Natl Acad Sci U S A 2017;114:E1737–44. https://doi.org/10.1073/pnas.1616866114.
Yentes JM, Hunt N, Schmid KK, Kaipust JP, McGrath D, Stergiou N. The appropriate use of approximate entropy and sample entropy with short data sets. Ann Biomed Eng 2013;41:349–65.
Zhang J, Huang Z, Chen Y, Zhang J, Ghinda D, Nikolova Y, et al. Breakdown in the temporal and spatial organization of spontaneous brain activity during general anesthesia. Hum Brain Mapp 2018;39:2035–46. https://doi.org/10.1002/hbm.23984.